Theoretical Study of a Steam-Ejector Refrigerator

Satha Aphornratana
Department of Mechanical Engineering
Sirindhorn International Institute of Technology,Thammasat University
Rangsit Campus, Klong Luang, Pathumthani 12121
THAILAND

ABSTRACT

This paper provides a theoretical analysis of a steam-ejector refrigerator. An ejector model is developed based on one-dimensional ideal gas theory which was first introduced by Keenan. This theory is modified to include losses associated with the primary nozzle, mixing chamber, and diffuser. This ejector model is then used to analyse thermodynamic performance of a steam ejector refrigeration cycle over a range of operating temperatures. The theoretical results are compared with the experimental results obtained from the literatures.

NOMENCLATURES

A	cross sectional area (m^2)	b	ejector exhaust (Fig. 2)
COP	Coefficient of Performance	*boiler*	boiler
h	specific enthalpy ($kJ.kg^{-1}$)	e	exit
k	specific heat ratio of an ideal gas,	*evap*	evaporator
m	mass flow rate ($kg.sec^{-1}$, $kg.min^{-1}$)	f	saturated liquid
M	Mach number	g	saturated vapor
P	absolute pressure (bar, mbar)	i	inlet, ideal
Q	heat energy (kJ, W)	o	stagnation state
R	gas constant ($kJ.kg^{-1}$, K^{-1})	p	primary (motive) fluid of an ejector
Rm	entrainment ratio of an ejector	s	secondary (entrained) fluid of an ejector
T	temperature (K, °C)	t	primary nozzle throat,
V	velocity ($m.sec^{-1}$)		
ρ	density ($kg.m^{-3}$)		
η_d	diffuser isentropic efficiency		
η_p	primary nozzle isentropic efficiency		
η_m	mixing chamber efficiency		

SUBSCRIPTS

1,2,3,...	see relevant figures

SUPERSCRIPTS

'	primary fluid
"	secondary fluid
*	condition at sonic velocity

1. INTRODUCTION

'A steam ejector refrigerator' was first developed by Le Blance & Parson around 1901 [1]. It experienced a wave of popularity during the early 1930's for air conditioning large buildings [2]. However, the steam ejector refrigerators were supplanted by systems using mechanical compressors.

Coefficient of Performance (*COP*) of a vapor compression system is normally greater than that of an ejector refrigerator. However, ejector refrigerators are similar to absorption refrigerators, they are powered by low grade temperature heat energy which is cheaper than mechanical power required by vapor compression systems.

Fig. 1 is a schematic diagram of an ejector refrigerator unit. As heat is added to the boiler, refrigerant vapor is evolved at a high pressure and temperature. This high pressure vapor, known as the primary fluid, expands through the primary nozzle of the ejector. Supersonic flow at low pressure is formed at the nozzle exit which entrains the secondary fluid from the evaporator. This low pressure allows liquid refrigerant, in the evaporator, to evaporate at low temperature to produce a refrigeration effect. The primary and secondary fluids are mixed in the mixing chamber of the ejector and discharged via the diffuser to the condenser, where the vapor is condensed. Part of the liquid refrigerant accumulated in the condenser is returned to the boiler via a pump whilst the remainder is expanded through the throttling valve to the evaporator, thus completing the cycle. The Coefficient of Performance (*COP*) of an ejector refrigerator is equal to the ratio between the heat absorbed by the evaporator (Q_{evap}) and the heat input to the boiler (Q_{boiler}). As the work input to the circulation pump is typically less than one percent of the heat supplied to the boiler, it is usually ignored, therefore:

$$COP = \frac{Q_{evapr}}{Q_{boiler}} \tag{1}$$

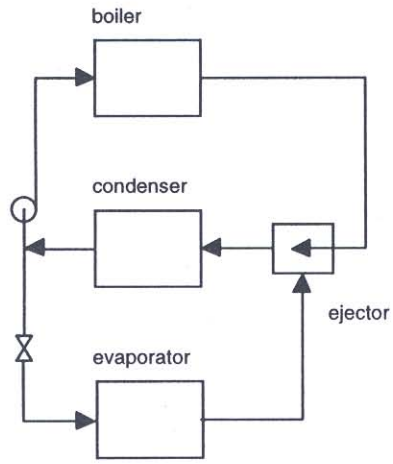

Fig. 1. An ejector refrigeration cycle.

In this paper, a steam-ejector model based on one-dimensional ideal gas dynamics is developed. It is used to analyse thermodynamic performance of a steam ejector refrigerator over a range of operating temperatures. The calculated results are compared with experimental data available in the literatures.

2. MODEL DESCRIPTIONS

A schematic view of a typical supersonic ejector is shown in Fig. 2. Referring to this figure; high pressure primary fluid (P) expands through the primary (supersonic) nozzle, producing a low pressure at the exit plane (1). This low pressure region draws and entrains the secondary fluid (S) into the mixing chamber. At the end of the mixing chamber (3), where it is assumed that these two streams are completely mixed and the flow speed is supersonic, a normal shock wave is induced creating a compression effect and the flow speed is reduced to subsonic. A further compression of the fluid is achieved as the flow passes through the subsonic diffuser section. The performance of an ejector is normally defined in terms of an entrainment ratio (R_m)which is defined as the ratio ($\dot{m}_s$) of the secondary to the primary fluid mass ($\dot{m}_p$) flow:

$$Rm = \frac{\dot{m}_s}{\dot{m}_p} \tag{2}$$

Some of the earliest researches on ejectors were carried out by Keenan & Neumann [3] who

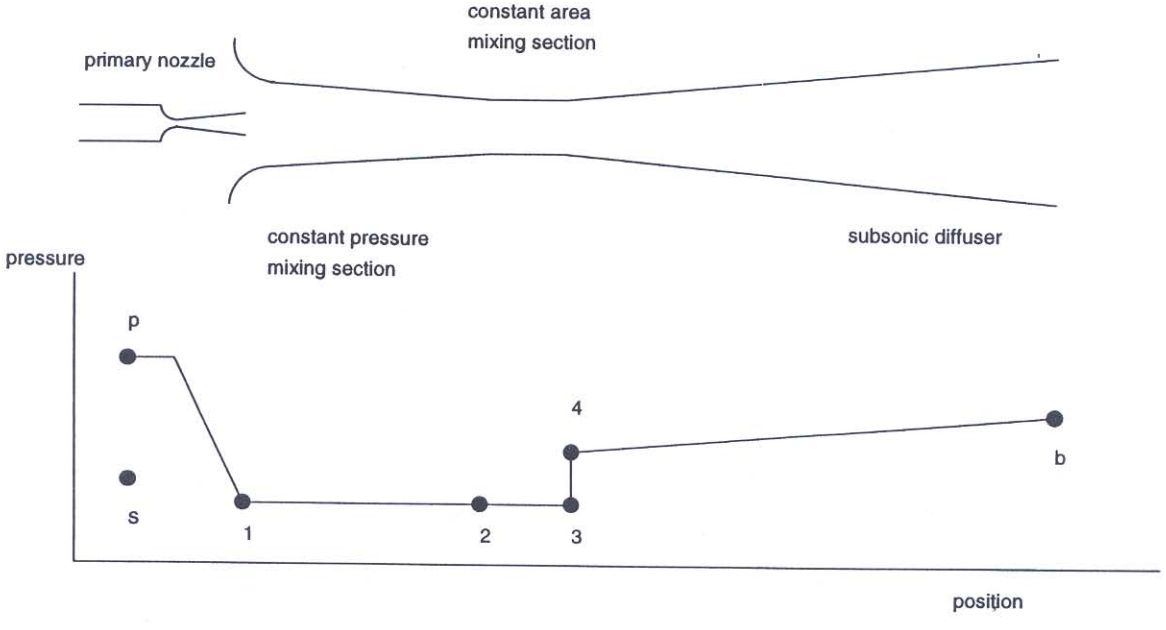

Fig. 2. An ejector.

undertook a theoretical analysis of an air ejector with a constant area mixing chamber and without a diffuser. They first developed a one-dimensional flow theory based on ideal gas dynamics in conjunction with the principles of mass, momentum, and energy conservation. The research was later extended to include a constant pressure mixing chamber and diffuser [4]. In order to eliminate analytical errors induced by the ideal gas assumptions, the thermodynamic properties of real gases may be applied. Such a model was developed by Stoecker [2]. However, in this study, it was found that both theories provided similar results. This was thought to be as a result of the low reduced pressure, thus, ideal gas assumptions model the properties of steam with reasonable accuracy. A computer model based on Keenan's theory was found to be more computationally efficient, therefore, this was selected for use.

Keenan's theory assumes isentropic flow. To overcome this problem isentropic efficiencies were applied to the primary nozzle, mixing, and diffusion processes. Values of isentropic efficiencies were selected to provide acceptable corrections between theoretical and experimental performance values reported in the literature. The analysis was based on the well known equations of energy, momentum, and mass flow continuity. The equations for a steady-flow process are given as:

Energy equation for adiabatic process:

$$\Sigma \dot{m}_i \left(h_i + h_i^2 / 2\right) = \Sigma \dot{m}_e \left(h_e + V_e^2 / 2\right) \tag{3}$$

Momentum equation:

$$P_i A_i + \Sigma \dot{m}_i V_i = P_e A_e + \Sigma \dot{m}_e V_e \tag{4}$$

Continuity equation:

$$\Sigma \rho_i V_i A_i = \Sigma \rho_e V_e A_e \tag{5}$$

Along with these governing equations, the following simplifying assumptions were included:

- Friction losses are introduced by applying appropriate efficiencies to the primary nozzle, diffuser, and mixing processes.
- The primary and secondary fluids are supplied at zero velocity at P and S respectively (Fig. 2).
- At the primary nozzle exit plane (1) where the two streams first meet, the static pressure is assumed to be uniform.
- Mixing of the two streams is completed before a normal shock wave occurs at the end of the mixing chamber (3).

2.1 Mach Number of the Primary Fluid at the Nozzle Exit Plane

Referring to Fig. 2; high pressure primary fluid at P expands through a converging-diverging nozzle leaving the nozzle at 1' with supersonic velocity. Applying energy equation between P and 1', the velocity at the nozzle exit is given as:

$$V_{1'}^2 = 2 \eta_p \left(h_p - h_{i,\,1'}\right) \tag{6}$$

where η_p is an isentropic efficiency of the primary nozzle. The relation between the pressure ratio across the nozzle and a form of Mach number at the nozzle exit is given as:

$$M_{1'}^{*} = \sqrt{\frac{2\,\eta_p}{k-1}\left[\left(\frac{P_p}{P_1}\right)^{\frac{k-1}{k}} - 1\right]} \tag{7}$$

2.2 Mach Number of the Secondary Fluid at the Nozzle Exit Plane

Referring to Fig. 2; as the low pressure is formed at the primary nozzle exit plane, the secondary fluid at S expands isentropically to 1". Similarly to the primary nozzle, the equivalent form of Mach number of the secondary fluid at the nozzle exit plane is given as:

$$M_{1''}^{*} = \sqrt{\frac{2}{k-1}\left[\left(\frac{P_s}{P_1}\right)^{\frac{k-1}{k}} - 1\right]} \tag{8}$$

2.3 Mixing Process in the Mixing Chamber

Referring to Fig. 2; applying the momentum equation between sections 1 and 3, results in:

$$\eta_m \left(P_1 A_1 + \dot{m}_p V_{1'} + \dot{m}_s V_{1''}\right) = P_3 A_3 + V_3 \left(\dot{m}_p + \dot{m}_s\right) \tag{9}$$

where η_m is the mixing chamber efficiency. In order to simplify the analysis, constant static pressure mixing process is assumed, and the cross section area at the inlet and exit of the mixing chamber are assumed to be equal. Thus, the velocity of the mixed fluid at 3 can be obtained from:

$$V_3 = \eta_m \left[\frac{\dot{m}_p V_{1'} + \dot{m}_s V_{1''}}{\dot{m}_p + \dot{m}_s}\right] \tag{10}$$

Eq. 10 can be written in terms of Mach number, therefore:

$$M_3^{*} = \eta_m \left[\frac{M_{1'}^{*} + Rm\, M_{1''}^{*} \sqrt{T_s / T_p}}{\sqrt{(1+Rm)\left(1 + RmT_s / T_p\right)}}\right] \tag{11}$$

where the relation between M and M^* is given as:

$$M^* = \sqrt{\frac{(k+1)(M^2/2)}{1+(k-1)(M^2/2)}} \tag{12}$$

2.4 Pressure Ratio Across a Normal Shock

At some section in the constant area mixing chamber (sections 2 to 4), a normal shock occurs, if the velocity of the mixed fluid entering the constant area section is supersonic. The shock wave is assumed to occur between sections 3 and 4. Mach number suddenly falls to less than unity. The Mach number of the mixed fluid after the shock wave is obtained from:

$$M_4 = \sqrt{\frac{M_3^2 + 2/(k+1)}{(2k/(k-1)M_3^2 - 1)}} \tag{13}$$

The pressure ratio across the shock wave is obtained from:

$$\frac{P_4}{P_3} = \frac{1 + kM_3^2}{1 + kM_4^2} \tag{14}$$

2.5 Pressure Ratio Across the Subsonic Diffuser

Further compression of the mixed fluid is achieved as it passes through the subsonic diffuser section. It is assumed that the flow speed is reduced to zero at the end of the diffuser (b). The pressure ratio across the diffuser can be obtained from:

$$\frac{P_b}{P_4} = \left[\frac{\eta_d (k-1)}{2} M_4^2 + 1\right]^{\frac{k}{k-1}} \tag{15}$$

where η_d is the isentropic efficiency of the diffuser.

2.6 Procedure to Solve P_b

If the temperatures, pressures and mass flows of the primary and secondary fluids are known, then the following procedure can be used to obtain the ejector exhaust pressure.

1. As the pressure at the nozzle exit plane is not known, it can be determined by an iteration process. First, the value of P_1 / P_s is assumed.
2. Calculate Mach number of the primary and secondary fluids at the nozzle exit plane M_1. and M_1. from Eqs. 7 and 8.
3. Calculate Mach number of the mixed fluid M_3 from Eqs. 11 and 12.
4. Calculate Mach number M_4 of the mixed fluid after the shock from Eq. 13.
5. Calculate a pressure ratio across the shock wave P_4 / P_3 from Eq. 14.

6. Calculate a pressure lift ratio across the diffuser P_b / P_4 from Eq. 15.
7. Now, the ejector exhaust pressure P_b can be calculated as P_4 / P_3, P_b / P_4, and P_1 / P_s are all known.
8. Repeat step 1 with new value of P_1 / P_s until the maximum P_b is obtained.

By trial and error, it was found that the values of 0.85, 0.85, and 0.95 for primary nozzle, diffuser, and mixing chamber efficiencies respectively were found to provide acceptable correlations with the experimental data provided by ESDU [5] as shown by Figs. 3 and 4. The best ESDU values shown in the figures represent the maximum achievable performance with state of the art designs, whilst the typical ESDU values represent average performance of conservative designs. It can be seen that, when all the loss factors are introduced, the calculated entrainment ratios agree well with the experimental values given in the literature. It is interesting to note that, at low primary pressure ratio the calculated performance is slightly higher than the experimental values, however, the difference between them is reduced as the primary pressure ratio increases. (The primary ratio is defined as the ratio of the primary fluid to the ejector exhaust pressure and the secondary pressure is defined as the ratio of the secondary fluid to the ejector exhaust pressures.) The primary pressure ratio (P_p / P_b) were typically greater than 50, e.g., at the boiler and condenser temperatures of 125 °C (2.32 bar) and 30 °C (42.5 mbar) respectively, the primary pressure ratio is 54.6:1. From these figures, it can be seen that, at high primary pressure ratios, the theoretical performance agrees well with the ESDU experimental values.

It was concluded from this that performance predictions based on modified Keenan's one-dimensional model should provide an accurate prediction of the performance of a steam ejector which is a critical part of steam ejector refrigerators.

3. PERFORMANCE OF A STEAM EJECTOR REFRIGERATOR

After obtaining the entrainment ratio, the Coefficient of Performance (COP) of a steam ejector refrigerator can be calculated from:

$$COP = Rm \left[\frac{h_{v,\,evap} - h_{f,\,con}}{h_{v,\,boiler} - h_{f,\,con}} \right] \tag{16}$$

Figs. 5 and 6 show the results of the calculated COP of a steam ejector refrigerator over a range of operating temperatures. The Coefficient of Performance value shown by the solid lines in these figures does not represent the value of a single cycle since any point on the lines requires a particular ejector (operated at its design condition). The ejector area ratio, defined as the ratio of the mixing chamber throat area (A_4) to the primary nozzle throat area (A_1), required for each operating condition is shown by dotted lines and obtained from Eq. 23 (refer to appendix). From the figures it can be concluded that:

- A steam ejector cycle which is designed to operate at high boiler and evaporator temperatures and low condenser temperatures will have higher COP values and require an ejector with larger area ratio than otherwise.
- For ejectors with the same area ratio and evaporator temperature, any rise in the boiler temperature causes the COP to fall, however, the cycle can be operated at a higher condenser temperature.
- For ejectors with the same area ratio and boiler temperature, an increase in the evaporator

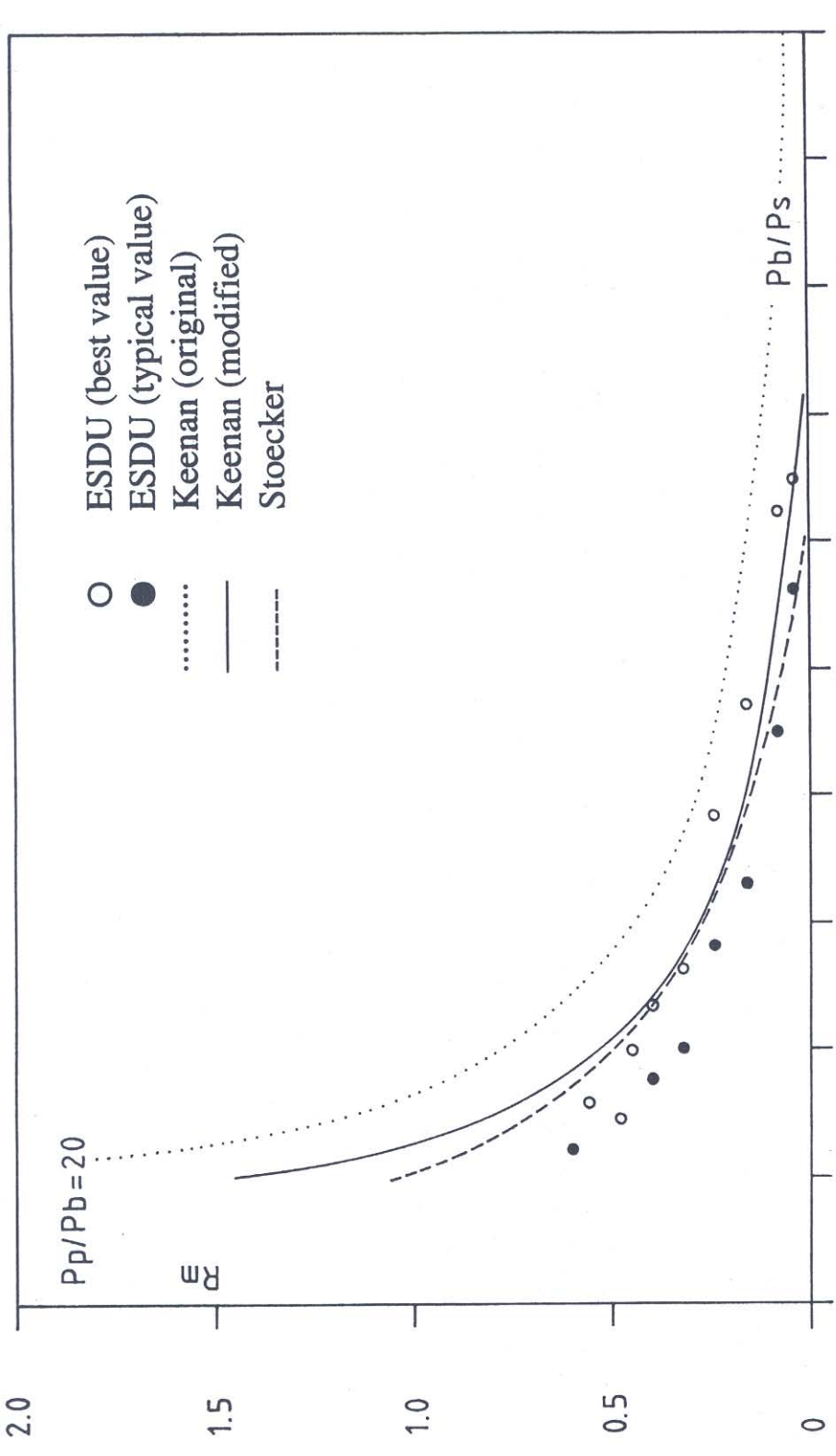

Fig. 3. Comparison between theoretical and experimental entrainment ratios (primary pressure ratio 20).

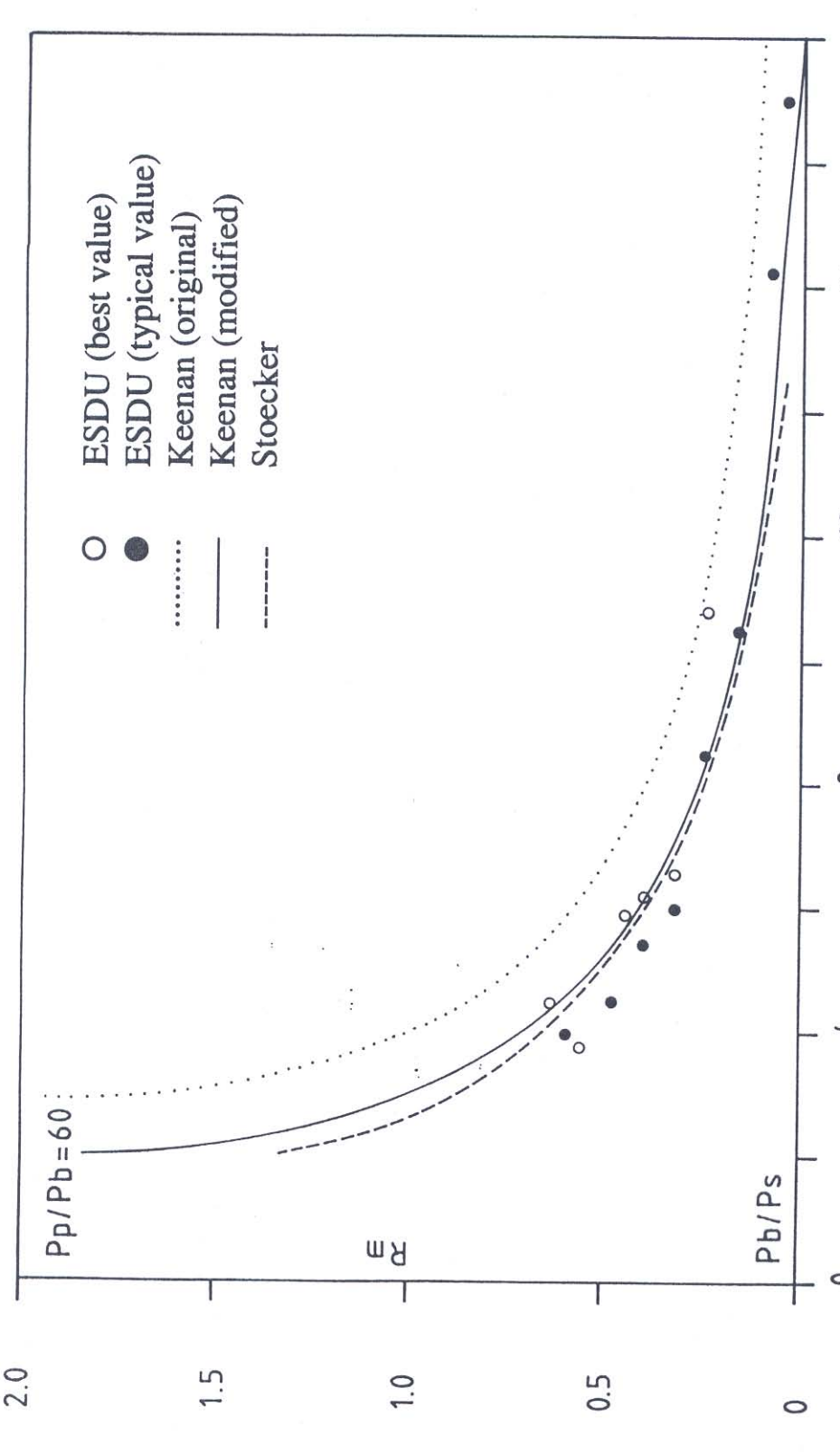

Fig. 4. Comparison between theoretical and experimental entrainment ratios (primary pressure ratio 60).

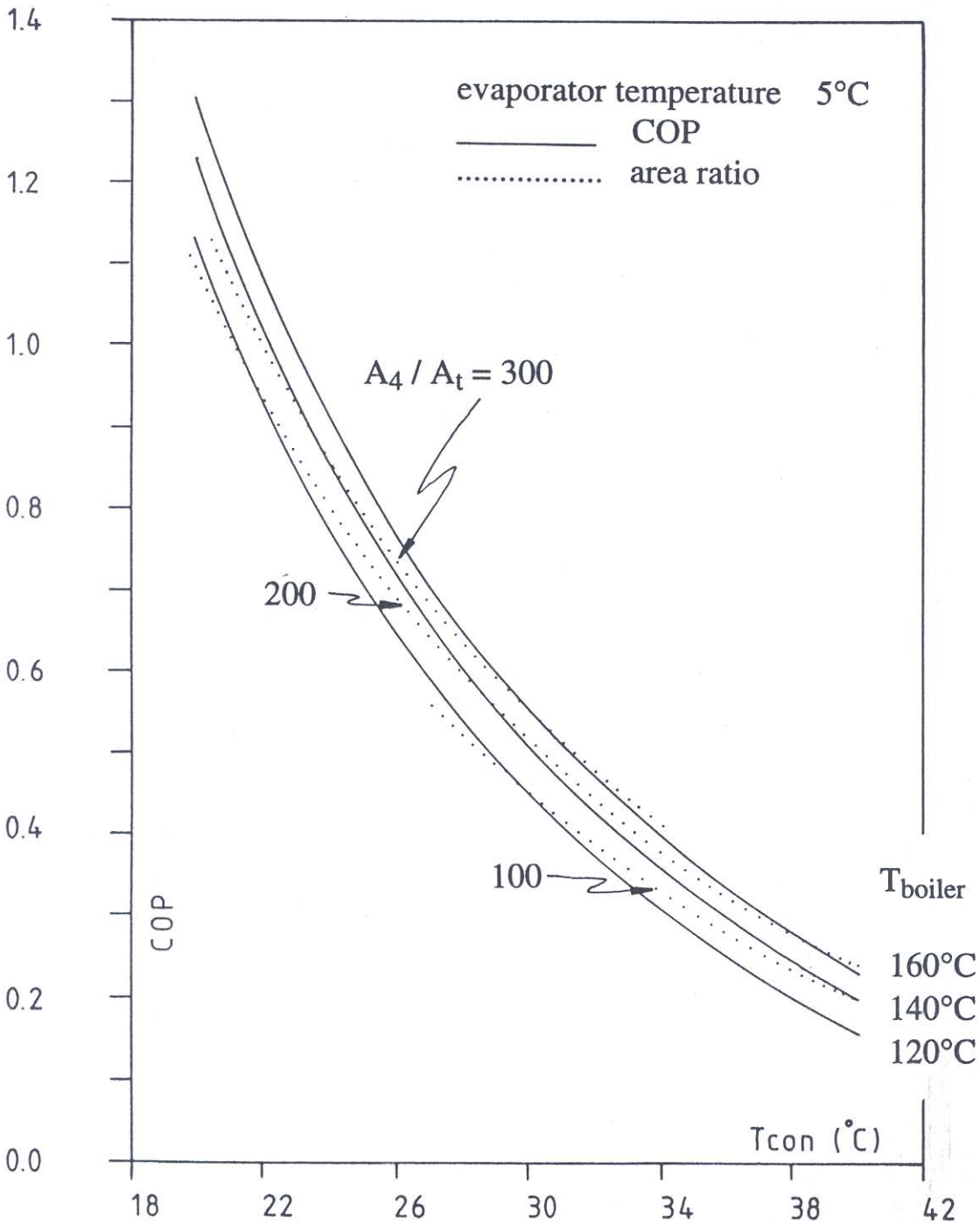

Fig. 5. Theoretical COP of a steam ejector refrigerator for fixed evaporator temperature and various boiler temperatures.

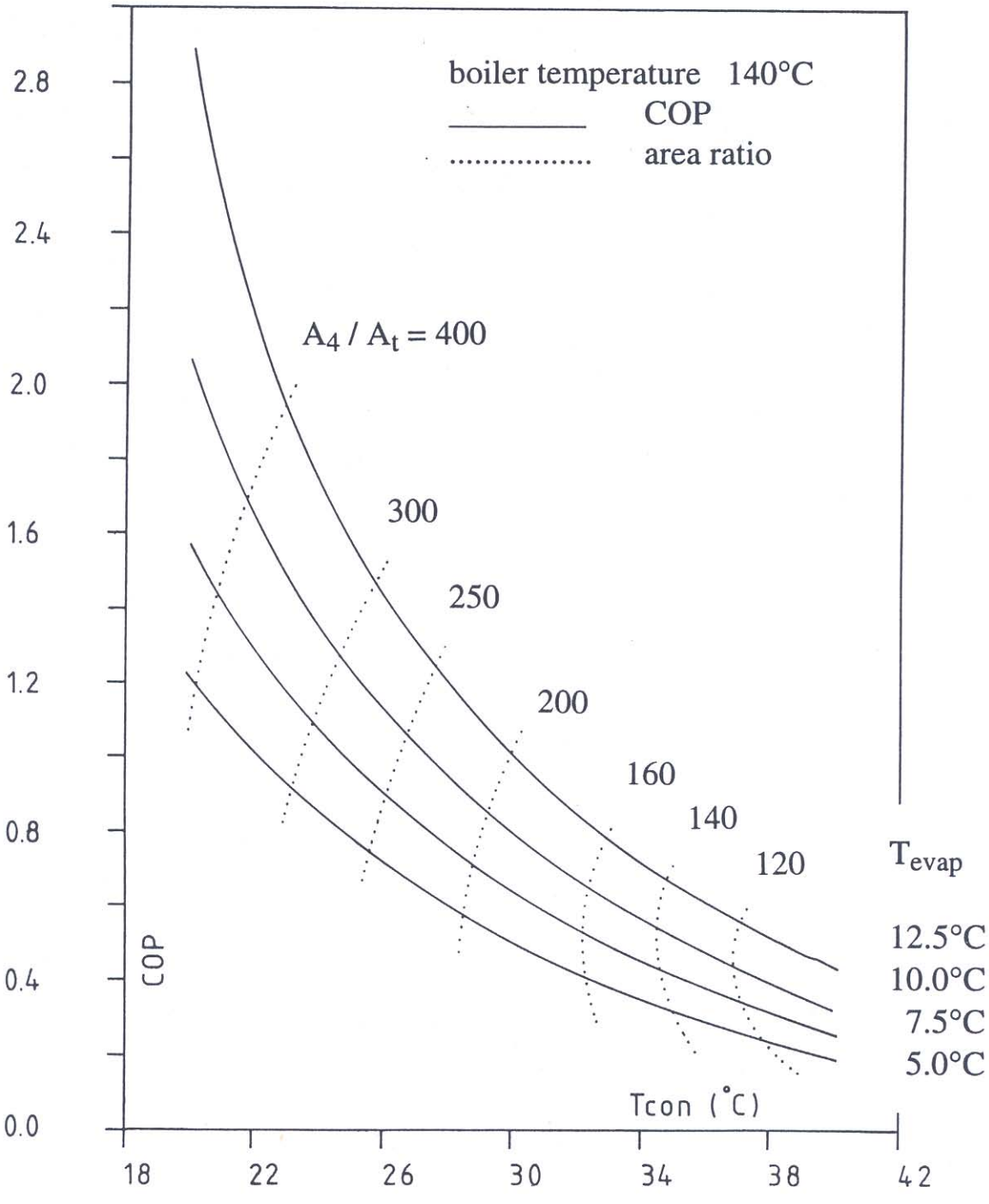

Fig. 6. Theoretical COP of a steam ejector refrigerator for fixed boiler temperature and various evaporator temperatures.

temperature causes the COP to rise and the cycle can be operated at higher condenser temperature.

A comparison between theoretical and the experimental results obtained from various sources provided by Munday and Bagster [6], are given in Table 1. It can be seen from this that most of the theoretical results agree well with the experimental values. Some of the theoretical results probably over estimated, because the ejectors used in the experiments may not have been operated at their design condition.

Table 1. Performance data of steam ejector refrigeration cycles.

A : experimental values reported in Munday and Bagster's paper [6]
B : theoretical values from modified Keenan's model

Investigator	Year	Temperature (°C)			Performance*(kJ/kg)		*COP*	
		Boiler	Con	Evap	A	B	A	B
Petzold	1950	184.3	35.2	1.0	520	705	0.197	0.268
		184.3	37.3	11.3	1090	1550	0.416	0.591
		184.3	38.5	17.6	1590	2384	0.607	0.910
		184.3	39.5	22.3	1980	3252	0.757	1.244
		165.5	31.8	18.5	2600	4274	0.981	1.626
Hammer	1951	124.0	31.4	19.0	2680	3862	1.038	1.498
		126.1	31.4	11.0	1610	1870	0.623	0.724
		127.2	31.4	9.0	1320	1573	0.511	0.610
		127.9	31.4	6.0	1160	1198	0.448	0.464
		128.7	31.4	3.0	890	898	0.344	0.347
		129.2	31.4	0.0	655	652	0.253	0.252
Stinson	1943	169.9	33.6	4.4	1200	1069	0.457	0.407
		169.9	33.6	7.2	1340	1382	0.510	0.527
		169.9	33.6	10.0	1600	1765	0.609	0.672
		169.9	38.7	7.2	1040	900	0.399	0.346
		169.9	38.7	12.8	1340	1490	0.514	0.572
		169.9	43.1	4.4	680	435	0.263	0.168
		169.9	43.1	10.0	1020	803	0.394	0.311
		169.9	43.1	12.8	1190	1049	0.460	0.404
		169.9	43.1	15.6	1370	1332	0.529	0.516
Jackson	1936	169.9	32.9	10.0	1900	1868	0.722	0.711
		169.9	40.8	10.0	1120	979	0.431	0.377
		169.9	36.7	15.6	2150	2212	0.822	0.847
		169.9	20.4	4.4	3200	3265	1.191	1.218
		169.9	42.4	4.4	620	469	0.239	0.181
		169.9	49.4	10.0	560	438	0.219	0.172
		169.9	42.4	15.6	1400	1408	0.540	0.544

* The performance is defined as a cooling capacity per unit of the motive steam.

4. CONCLUSIONS

A steam-ejector model based on Keenan's theory was modified to include irreversibilities associated with primary nozzle, mixing chamber, and diffuser. The model was used to predict performance of steam ejector and the results were compared with the experimental data. It was found that, the calculated results agreed well with the experimental data. This ejector model was used to study thermodynamic performance of steam-ejector refrigerator. The study showed that, thermodynamic performance of a steam-ejector depended on boiler, condenser, and evaporator temperature. The area ratio (primary nozzle throat / mixing chamber throat) is also important.

5. REFERENCES

1. ASHRAE. 1983. *ASHRAE Handbook: Equipment Volume*. s. l.:ASHRAE.
2. Stoecker, W. F. 1958. *Refrigeration and Air Conditioning*. New York: McGraw-Hill.
3. Keenan, J. H., and Neumann, E. P. 1942. A simple air ejector. *ASME J. Applied Mechanics* June: A75-81.
4. Keenan, J. H.; Neumann, E. P. and Lustwerk, F. 1950. An investigation of ejector design by analysis and experiment. *ASME J. Applied Mechanics* Sept.: 299-309.
5. ESDU. 1985. *Ejector and Jet Pump, Data Item 8603*. London: ESDU International Ltd.
6. Munday, J. T., and Bagster, D. F. 1977. A new ejector theory applied to steam jet refrigeration. *Ind. Eng. Chem.* Process Des. Div. 16 (4): 442-449.

6. APPENDIX: CROSS-SECTIONAL AREA OF AN EJECTOR

To relate the cross-sectional area of an ejector, the continuity equation is used:

$$A = \frac{m}{\rho V} \tag{17}$$

Applying the ideal gas law to Eq. 17 gives:

$$A = \frac{\dot{m}}{M\sqrt{k\,R\,T_o}}\left[\frac{R\,T_o}{P_o}\right]\left[\frac{P}{P_o}\right]^{1/k} \tag{18}$$

where subscript "*o*" denotes the stagnation condition. The geometry of each region of an ejector (Fig. 2) may, therefore, be characterized non-dimensionally as a cross-sectional area ratio by normalization with that of the primary nozzle throat.

Primary nozzle throat

$$A_t = \frac{\dot{m}_p}{P_p}\sqrt{\frac{T_p\,R}{k}\left[\frac{k+1}{2}\right]^{\frac{k+1}{k-1}}} \tag{19}$$